M.V. Yarmolenko

Copper and Aluminum Electric Corrosion Investigation and Intermetallics Disappearance in Cu-Al System Analysis

Kyiv National University of Technologies and Design, Faculty of Market, Information and Innovation Technologies, Cherkasy, Ukraine, yarmolenko.mv@knutd.edu.ua

Copper and aluminum electric corrosion is investigated experimentally. It is founded that copper corrosion is higher than aluminum corrosion. Intermetallics disappearance rate in Cu-Al system is analyzing theoretically. Literature experimental data are used for analysis.

Key words: copper, aluminum, electrolysis, diffusion, intermetallics, phases formation kinetics.

Introduction

Mutual diffusion in β-phase ($C_{Al} \approx 0.24 \pm 0.02$) of Cu-Al system was investigated at temperatures from 700 ^{o}C to 840 ^{o}C (β-phase can exist at temperatures that are higher than 565 ^{o}C) [1]. The phase formation kinetics between α-phase ($C_{Al} \approx 0.15$) and γ-phase ($C_{Al} \approx 0.31$) was analyzed, and β-phase formation kinetics between pure copper (99.99 % Cu) and γ-phase ($C_{Al} \approx 0.31$) was analyzed too. The phase formation parabolic law was observed. The pre-exponential factor and mutual diffusion activation energy for diffusion in β-phase were calculated: $D_0 \approx 1.3 \cdot 10^{-5} \ m^2/s$, $Q \approx 27 \pm (3 \div 5)$ kcal/mol. The pre-exponential factor and β-phase formation activation energy were calculated: $D_0 \approx 10^{-2} \div 10^{-1} \ m^2/s$, $Q \approx 40 \pm 3$ kcal/mol. It was proved experimentally that mutual diffusion penetrability of β-phase does not depend on annealing time and initial composition. It was proved experimentally [2] that copper corrosion rate is higher than gold corrosion rate, but intermetallics formation rate in Au-Al system is much more higher than intermetallics formation rate in Cu-Al system, so it is possible to use Cu instead of Au for wire bonding in microelectronics packaging, because thin Al pad (1.2 μm thickness) can prevent gold and copper corrosion, and Cu has higher electric conductivity, higher thermal conduction, and lower material cost than Au. Theoretical method was proposed to describe intermetallics disappearance rate in double multiphase systems [3].

Another theoretical method was described to calculate intermetallics formation rate in double multiphase systems [4]. Three phases growth kinetics (ε-brass, CuZn$_5$, $C_1 \approx 0.83$; γ-brass, Cu$_5$Zn$_8$, $C_2 \approx 0.62$; and β-brass, CuZn, $C_3 \approx 0.5$) was analyzed theoretically and experimentally at 230 ^{o}C, 340 ^{o}C, and 400 ^{o}C in planar and cylindrical samples [5, 6, 13, 14], and theoretically in spherical samples [15].

Electric current can destruct wire bonding in microelectronics packaging, so we planned to investigate copper and aluminum electric corrosion. Direct current can dissolve metal anode into electrolyte, and we planned to do experiments under the same conditions: initial radii of Al and Cu anodes should be equal; electrolyte concentration should be the same; anodes lengths immersed into electrolyte should be approximately equal; graphite cathodes should be the same; direct electric current value should be practically the same.

I. Experimental results of copper and aluminum electric corrosion investigation

Cylindrical anodes (99.99 % Cu and 99.99 % Al) were used for copper and aluminum electric corrosion investigation. Sodium chloride (NaCl) solution was used as electrolyte (Fig. 1). Direct electric current and anodes
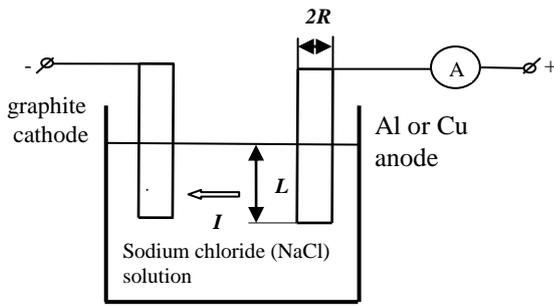
Fig. 1. Scheme of experimental equipment.

mass decreasing were measured. First of all, we need to be assured that ions Cu^+ (or Cu^{2+}) and Al^{3+} were present in NaCl solution. Rate of anode dissolving into electrolyte can be calculated using Faraday's law of electrolysis:

$$\frac{dm}{dt} = \frac{MI}{zF}, \quad dm = \rho \cdot L \cdot \pi \cdot d(R^2(t)), \quad (1)$$

where m is anode mass dissolved into electrolyte, t is time of experiment, M is molar mass, I is direct electric current value, F is the Faraday constant ($F = 96485.33289(59)$ C mol^{-1}), z is charge of ions, R is anode radius, L is anode length immersed into electrolyte. Electric current value did not change, so one can calculate:

$$z = \frac{MIt}{F\pi\rho L(R^2(t=0) - R^2(t))}, \quad (2)$$

where ρ is anode density. Charges of copper and aluminum ions were calculated:

$$z_{Cu} = \frac{63.55 \cdot 10^{-3}\,kg/mol \cdot 2.8A \cdot 1.2 \cdot 10^3\,s}{F \cdot \pi \cdot 8.9 \cdot 10^3\,kg/m^3\,L_{Cu} \cdot (R_{Cu}^2(t=0) - R_{Cu}^2(t_4))} \approx 0.995 \approx 1, \quad (3)$$

$$z_{Al} = \frac{27 \cdot 10^{-3}\,kg/mol \cdot 3.1A \cdot 1.2 \cdot 10^3\,s}{F \cdot \pi \cdot 2.7 \cdot 10^3\,kg/m^3\,L_{Al} \cdot (R_{Al}^2(t=0) - R_{Al}^2(t_4))} \approx 2.954 \approx 3, \quad (4)$$

where $L_{Cu} \approx L_{Al}$: $L_{Cu} = 5 \cdot 10^{-2}$ m, $L_{Al} = 4.5 \cdot 10^{-2}$m; $R_{0Cu} = R_{0Al} = 2.8$ m; $I_{Al} \approx I_{Cu}$: $I_{Al} = 3.1$ A, $I_{Cu} = 2.8$ A, so copper dissolved into NaCl solution as Cu^+ ions, and aluminum dissolved into NaCl solution as Al^{3+} ions. Anodes radii decreasing kinetics is shown on Fig.2. Experiments were carried during $t_1 = 5$ min, $t_2 = 10$ min, $t_3 = 15$ min, and $t_4 = 20$ min. Experimental results are as follows: $R_{1Cu} = 2.74$ mm, $R_{2Cu} = 2.67$ mm, $R_{3Cu} = 2.59$ mm, $R_{4Cu} = 2.5$ mm; $R_{1Al} = 2.77$ mm, $R_{2Al} = 2.73$ mm, $R_{3Al} = 2.68$ mm, $R_{4Al} = 2.62$ mm. Measurement precision was 0.01 mm.

Chemical reactions took place near positive electrode (anode):

$$Cu^+ + Cl^- = CuCl \downarrow,$$
$$Al^{3+} + 3Cl^- = AlCl_3 \downarrow,$$
$$Cu^+ - e^- = Cu^{2+},$$
$$Cu^{2+} + 2Cl^- = CuCl_2 \downarrow, \quad (5)$$
$$Cl^- - e^- = Cl^0, \quad Cl^0 + Cl^0 = Cl_2 \uparrow.$$
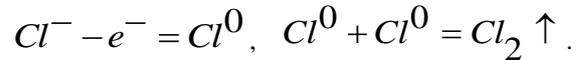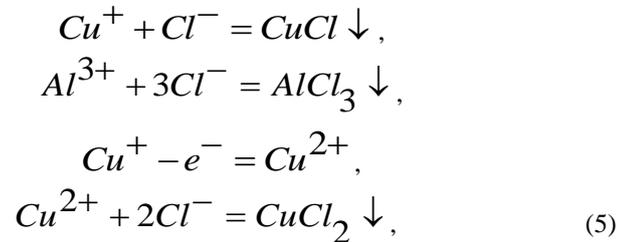
Chlorine gas was formed near anode.

Chemical reactions took place near negative electrode (cathode):

$$Na^+ - e^- = Na^0,$$
$$2Na + 2H_2O = 2NaOH + H_2 \uparrow. \quad (6)$$
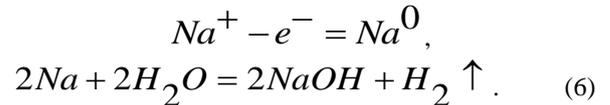
Hydrogen gas was formed near anode.

Anodes radii decreasing rate constants can be calculated as average value of four experiments:

$$k_{Cu} = \frac{4R_0^2 - \sum_{i=1}^{4} R_i^2}{\sum_{i=1}^{4} t_i} \approx 1.25 \cdot 10^{-9}\,m^2/s, \quad (7)$$

Fig. 2. Al and Cu anodes radii decreasing kinetics.

$$k_{Al} = \frac{4R_0^2 - \sum\limits_{i=1}^{4} R_i^2}{\sum\limits_{i=1}^{4} t_i} \approx 7.29 \cdot 10^{-10} \, m^2\!/\!s \ ,$$

$$k_{Cu} \approx 1,72 k_{Al} \ , \tag{8}$$

so copper electric corrosion is much more higher than aluminum electric corrosion, despite of $I_{Al} \geq I_{Cu}$: $I_{Al} \approx 1.1 \, I_{Cu}$. It is need to point out that k_{Cu} and k_{Al} have dimensionalities as diffusion coefficient because the anodes had cylindrical shape.

II. Analysis of intermetallics disappearance rate in Al-Cu system

There are three phases in Cu-Al system at temperatures from 175 °C to 225 °C [2]: CuAl$_2$ ($C_1 = 2/3 \approx 0.67$), CuAl ($C_2 = \frac{1}{2} = 0.5$), and γ-phase Cu$_9$Al$_4$ ($C_3 = 4/13 \approx 0.31$), $C = C_{Al}$. Phases 1, 2, and 3 formation rates between thin Al layer and Cu can be calculated, using so-called "constant flux method" (K.P. Gurov and A.M. Gusaks' method) [4]:

$$\frac{dX_1}{dt} \approx \frac{1-C_2}{(1-C_1)(C_1-C_2)}\frac{D_1}{X_1} - \frac{1}{C_1-C_2}\frac{D_2}{X_2} = \frac{K_1}{2X_1}, \quad X_1^2 = K_1 t ,$$

$$\frac{dX_2}{dt} \approx \frac{C_1-C_3}{(C_1-C_2)(C_2-C_3)}\frac{D_2}{X_2} - \frac{1}{C_1-C_2}\frac{D_1}{X_1} - \frac{1}{C_2-C_3}\frac{D_3}{X_3} = \frac{K_2}{2X_2}, \tag{9}$$

$$X_2^2 = K_2 t , \quad \frac{dX_3}{dt} \approx \frac{C_2}{C_3(C_2-C_3)}\frac{D_3}{X_3} - \frac{1}{C_2-C_3}\frac{D_2}{X_2} = \frac{K_3}{2X_3}, \quad X_3^2 = K_3 t ,$$

$$(X_1 + X_2 + X_3)^2 = X^2 = K_{123} t , \quad K_{123} = \left(\sqrt{K_1} + \sqrt{K_2} + \sqrt{K_3}\right)^2 ,$$

where D_i ($i = 1; 2; 3$) is mutual diffusion penetrability of phase i ($D_i = D_i^* \cdot \Delta C_i$), D_i^* is mutual diffusion coefficient in phase i, ΔC_i is narrow concentration range of homogeneity. K_1 depends on D_1 and D_2, K_2 depends on D_1, D_2 and D_3, and K_3 depends on D_3 and D_2. Aluminum disappearance time, t_0, can be estimated by the following way. Mass conservation law gives (Fig. 3):

$$X_{Al}(t=0) \cdot 1 = C_1 X_1(t_0) + C_2 X_2(t_0) + C_3 X_3(t_0) =$$

$$= C_1\left(\sqrt{K_1} + \frac{C_2}{C_1}\sqrt{K_2} + \frac{C_3}{C_1}\sqrt{K_3}\right)\sqrt{t_0} \approx C_1\sqrt{K_{123}}\sqrt{t_0} ,$$

and

$$t_0 = \frac{X_{Al}^2}{(C_1\sqrt{K_1} + C_2\sqrt{K_2} + C_3\sqrt{K_3})^2} \approx \frac{X_{Al}^2}{C_1^2 K_{123}} . \tag{11}$$

Two phases (phase 2 and phase 3) are formed between phase 1 and copper after disappearance of aluminum:
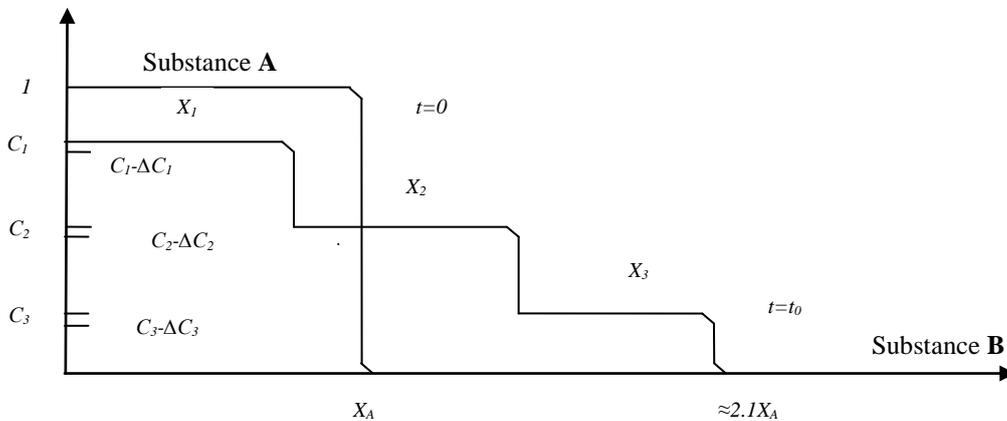
Fig. 3. Concentration profile change during isothermal annealing from $t = 0$ to $t = t_0$.

$$\frac{dX_2}{dt} \approx \frac{C_1 - C_3}{(C_1 - C_2)(C_2 - C_3)} \frac{D_2}{X_2} - \frac{1}{C_2 - C_3} \frac{D_3}{X_3} = \frac{K_2}{2X_2}, \quad X_2^2 = K_2 t,$$

$$\frac{dX_3}{dt} \approx \frac{C_2}{C_3(C_2 - C_3)} \frac{D_3}{X_3} - \frac{1}{C_2 - C_3} \frac{D_2}{X_2} = \frac{K_3}{2X_3}, \quad X_3^2 = K_3 t, \tag{12}$$

$$(X_2 + X_3)^2 = X^2 = K_{23}t, \quad K_{23} = \left(\sqrt{K_2} + \sqrt{K_3}\right)^2 \approx \frac{4}{9} K_{123}, \text{ if } K_1 \approx K_2 \approx K_3.$$

Mass conservation law gives (Fig. 4):

$$X_{Al}(t=0)\cdot 1 = C_2 X_2(t_1) + C_3 X_3(t_1) = \sqrt{t_1} C_2 (\sqrt{K_2} + \frac{C_3}{C_2}\sqrt{K_3}),$$

and
$$t_1 \approx \frac{X_{Al}^2}{C_2^2 K_{23}} \approx \frac{9 X_{Al}^2}{4 C_2^2 K_{123}}. \tag{13}$$
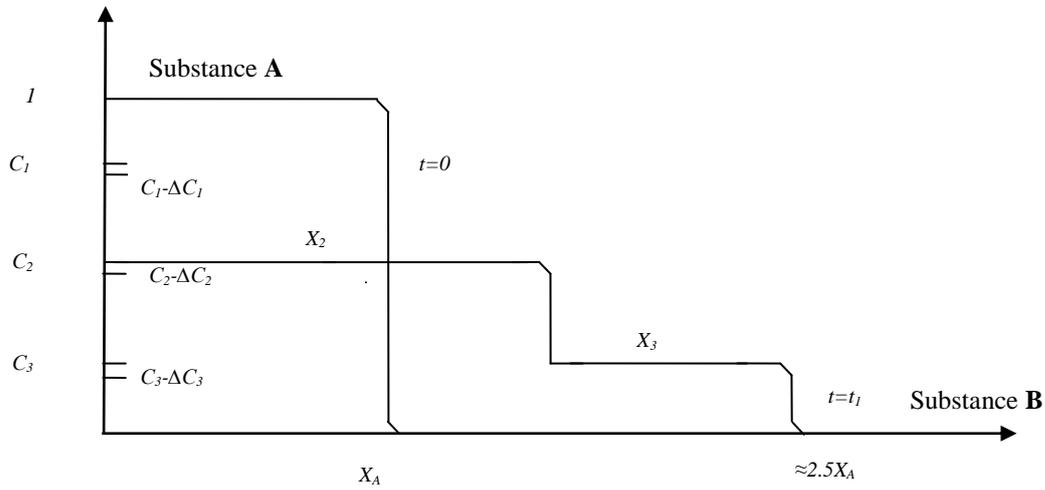
Fig. 4. Concentration profile change during isothermal annealing from $t=0$ to $t=t_1$.

Phase 3 is formed between phase 2 and copper after disappearance of aluminum and phase 1:

$$\frac{dX_3}{dt} \approx \frac{C_2}{C_3(C_2 - C_3)} \frac{D_3}{X_3} = \frac{K_3}{2X_3}, \quad X_3^2 = K_3 t \approx \frac{1}{9} K_{123} t. \tag{14}$$

Mass conservation law gives (Fig. 5):

$$X_{Al}(t=0)\cdot 1 = C_3 X_3(t_2) = \sqrt{t_2} C_3 \sqrt{K_3}, \text{ and}$$

$$t_2 \approx \frac{X_{Al}^2}{C_3^2 K_3} \approx \frac{9 X_{Al}^2}{C_3^2 K_{123}}. \tag{15}$$
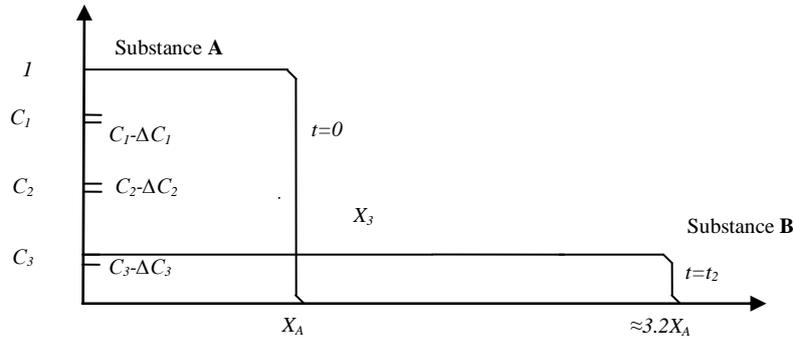
Fig. 5. Concentration profile change during isothermal annealing from $t = 0$ to $t = t_2$.

We can analyze described experimental results [2]. The Au and Cu wires were bonded to the Al/0.5% Cu pad of $X_{Al} = 1.2$ µm thickness using the ASM Eagle 60AP wire bonder. The Au and Cu wires were annealing at temperatures $T_1 = 175$ °C, $T_2 = 200$ °C, and $T_3 = 225$ °C during 120 h, 240 h, 360 h and 480 h. Phase layers thicknesses for Cu/Al were calculated:

$$X^2 = K_{123}t + K_{01} = 3.52 \cdot 10^{-4}\ \mu m^2\!/\!s \cdot e^{(-3064.5/T)}t + 0.44\mu m^2,$$

where K_{01} is constant related to initial IMC thickness. General reaction rates of IMC formation were calculated: $K_{123}(T_1) = 3.57 \cdot 10^{-7}$ µm²/s, $K_{123}(T_2) = 6.26 \cdot 10^{-7}$ µm²/s, $K_{123}(T_3) = 7.15 \cdot 10^{-7}$ µm²/s. The pre-exponential factor and IMC formation activation energy were calculated: $K_0 \approx 3.52 \cdot 10^{-4}$ µm²/s, $Q \approx 6.1$ kcal/mol. We can calculate aluminum disappearance time for different temperatures using Equation (11):

$$t_0(T_1) \approx 2520\,h, \quad t_0(T_2) \approx 1440\,h,$$

$$t_0(T_3) \approx 1260h, \quad t \approx \frac{480h}{1260h}t_0 \approx 0.4t_0,$$

so all three phases are formed in diffusion zone (Fig. 6):

$$X_A(t = 0.4t_0) \approx C_1\sqrt{K_{123}t_0}\sqrt{1 - 0.4} \approx 0.77 X_A(t = 0)\ .(16)$$
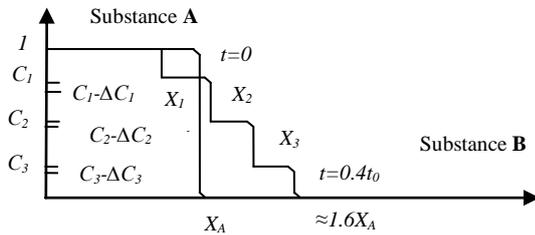
Fig. 6. Concentration profile change during isothermal annealing in Al-Cu system from $t=0$ to $t=0.4t_0$.

Phase 1 disappearance time at temperature T_3 can be calculated using Equation (13):

$$t_1(T_3) \approx 5035h \approx 7 months.$$

Phase 2 disappearance time can be calculated using Equation (15):

$$t_2(T_3) \approx 52390h \approx 6 years.$$

By the way, assumption $K_1 \approx K_2 \approx K_3$ is incorrect [5, 6, 13], so obtained estimations should be less in several times. Equations (11), (13), and (15) correctly describe obtained experimental results [5, 6].

Conclusions

Copper electric corrosion is much more higher than aluminum electric corrosion, $k_{Cu} \approx 1,72k_{Al}$, so thin Al pad can prevent copper electric corrosion. Anodes radii decreasing rate constants, k_{Cu} and k_{Al}, have dimensionalities as diffusion coefficient, because the anodes had cylindrical shape.

Thin metal covering disappearance time, t_0, can be estimated by the following way:

$$t_0 = \frac{X_A^2}{(C_1\sqrt{K_1} + C_2\sqrt{K_2} + C_3\sqrt{K_3})^2} \approx \frac{X_A^2}{C_1^2 K_{123}},$$

where X_A is initial metal covering thickness, C_1 is concentration in phase 1, K_{123} is general reaction rates of IMC formation, $C_1 > C_2 > C_3$; K_1, K_2, and K_3 are phases 1, 2, and 3 formation rates.

Phase 1 disappearance time, t_1, can be calculated:

$$t_1 \approx \frac{X_A^2}{C_2^2 K_{23}} \approx \frac{9 X_A^2}{4 C_2^2 K_{123}}.$$

Phase 2 disappearance time, t_2, can be calculated:

$$t_2 \approx \frac{X_A^2}{C_3^2 K_3} \approx \frac{9 X_A^2}{C_3^2 K_{123}}.$$

It is need to point out that K.P. Gurov and A.M.Gusaks' method can be applied to describe phase formation rate along GB with outflow in volume [7, 8, 9]

(J.C.Fisher's model [10]) and along dislocation pipe with outflow in volume [11] (A.D. LeClaire and A. Rabinovichs' model [12]).

Yarmolenko M.V. - PhD, Associate Professor, Head of the Chair of Information and Computer Technologies and Fundamental Disciplines.

[1]   V.N. Pimenov, K.A. Akkushkarova, and Yu.E. Ugaste, Fizika metallov i metalloved. 39(4) 821 (1975).
[2]   C.S. Goh, W.L.E. Chong, T.K. Lee, and C. Breach, Crystals 3, No.3, 391 (2013) (https://doi.org/10.3390/cryst3030391).
[3]   V.I. Neverov, Yu.E. Ugaste, Fizika i Khimia obrabotki materialov 5, 113 (1992).
[4]   K.P. Gurov, A.M. Gusak, and M.V. Yarmolenko, Metallofizika 10(3) 91 (1988) (https://mfint.imp.kiev.ua/ru/toc/v10/i05.html).
[5]   V.V. Bogdanov, A.M. Gusak, L.N. Paritskaya, and M.V. Yarmolenko, Metallofizika 12(3) 60 (1990).
[6]   V.V. Bogdanov, L.N. Paritskaya, and M.V. Yarmolenko, Metallofizika 12(5) 98 (1990).
[7]   M.V. Yarmolenko, A.M. Gusak, and K.P. Gurov, Journal of Engineering Physics and Thermophysics 65, 876 (1993) (https://doi.org/10.1007/BF00862930).
[8]   M.V. Yarmolenko, Defect and Diffusion Forum 143-147, 1567 (1997) (https://doi.org/10.4028/www.scientific.net/DDF.143-147.1567).
[9]   M.V. Yarmolenko, Metallofiz. Noveishie Tekhnol. 40(9), 1201 (2018) (DOI: 10.15407/mfint.40.09.1201).
[10] J.C. Fisher, J. Appl. Phys. 22(1), 1699825 (1951) (https://doi.org/10.1063/1.1699825).
[11] M.V. Yarmolenko, AIP Advances 8, 095202 (2018) (https://doi.org/10.1063/1.5041728).
[12] A.D. Le Claire and A. Rabinovich, J. Phys. C: Solid State Phys. 15, 5727 (1982) (https://iopscience.iop.org/article/10.1088/0022-3719/15/16/007).
[13] A.M. Gusak and M.V. Yarmolenko, J. Appl. Phys. 73(10), 4881 (1993) (https://doi.org/10.1063/1.353805).
[14] M.V. Yarmolenko, Deviation from Parabolic Growth of Phase Layers in Cylindrical and Spherical Samples: Curvature and Internal Stress Influence in Proceedings of PTM-1994, W.C. Johnson, J.M. Howe, D.E. Laughlin, and W.A. Soffa (The Minerals, Metals & Materials Society, Pennsylvania, 1994), p.1177 (https://publons.com/publon/3639123/).
[15] M.V. Yarmolenko, Izvestiya AN SSSR. Metally 3, 187 (1990) (https://publons.com/publon/2915981/).

М.В. Ярмоленко

Дослідження електричної корозії міді і алюмінію та аналіз кінетики зникнення інтерметалідів у системі Cu-Al

Київський національний університет технології і дизайну, Черкаси, Україна, yarmolenko.mv@knutd.edu.ua

Експериментально досліджено електричну корозію міді та алюмінію. Отримано такий результат: електрична корозія міді значно швидша, ніж електрична корозія алюмінію, тому тонке алюмінієве покриття товщиною близько 1 мікрометра на мідних дротинках може уповільнити корозію міді у приладах мікроелектроніки. Теоретично проаналізовано процес зникнення інтерметалідів у системі Cu-Al. Для аналізу були використані літературні експериментальні дані.

Ключові слова: мідь; алюміній; електроліз; дифузія; інтерметаліди; кінетика утворення фаз.